Journal of Medicinal Chemistry

Brief Article

pubs.acs.org/jmc

Discovery of Potent Heterodimeric Antagonists of Inhibitor of Apoptosis Proteins (IAPs) with Sustained Antitumor Activity

Heidi L. Perez,* Charu Chaudhry, Stuart L. Emanuel, Caroline Fanslau, Joseph Fargnoli, Jinping Gan, Kyoung S. Kim, Ming Lei, Joseph G. Naglich, Sarah C. Traeger, Ragini Vuppugalla, Donna D. Wei, Gregory D. Vite, Randy L. Talbott, and Robert M. Borzilleri

Bristol-Myers Squibb Research, P.O. Box 4000, Princeton, New Jersey 08543, United States

Supporting Information

ABSTRACT: The prominent role of IAPs in controlling cell death and their overexpression in a variety of cancers has prompted the development of IAP antagonists as potential antitumor therapies. We describe the identification of a series of heterodimeric antagonists with highly potent antiproliferative activities in cIAP- and XIAP-dependent cell lines. Compounds **15** and **17** further demonstrate curative efficacy in human melanoma and lung cancer xenograft models and are promising candidates for advanced studies.

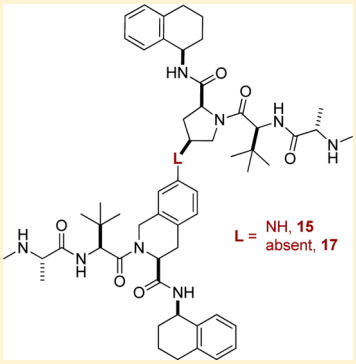

INTRODUCTION

Apoptosis is a highly regulated cell suicide process that results in the elimination of unwanted cells from multicellular organisms. Defects in apoptotic signaling can upset the balance between cell proliferation and cell death and lead to diseases such as cancer.[1] Elevated expression of antiapoptotic proteins is further associated with resistance to chemotherapeutic agents.[2] As such, the development of targeted therapies that induce apoptosis or sensitize tumor cells to cytotoxic agents is a promising strategy for the treatment of cancer.[3]

Inhibitor of apoptosis proteins (IAPs) are important regulators of apoptosis due to their ability to inhibit caspases. IAPs are characterized by the presence of at least one baculovirus IAP repeat (BIR) domain, which is essential for their antiapoptotic activity.[4] The third BIR domain (BIR3) of X-linked IAP (XIAP) binds to and inhibits caspase-9, while the second BIR domain (BIR2), together with the preceding linker region, binds to caspase-3 and -7.[5,6] In addition to direct inhibition of caspase-3, -7, and -9 by XIAP, cellular IAP1 and 2 (cIAP1/2) block TNF-α-mediated activation of caspase-8.[7] More recently, cIAPs have been shown to mediate canonical and noncanonical NF-κB signaling via ubiquitination of RIP1 and NIK, respectively.[8]

Second mitochondria-derived activator of caspases (Smac) (also known as direct IAP-binding protein with a low p*I*, DIABLO) is an endogenous, mitochondrial protein that antagonizes IAPs via a conserved *N*-terminal tetrapeptide motif (AVPI).[9,10] Homodimeric Smac competes with caspase-3, -7, and -9 for binding to the BIR2 and BIR3 domains of XIAP.[11,12] Binding of Smac to the BIR3 domain of cIAPs results in their rapid ubiquitination and proteasomal degradation, thereby releasing inhibition of caspase-8.[13] As IAPs are frequently overexpressed in human tumors, numerous IAP inhibitors have been developed based on the AVPI sequence of Smac.[14,15] Of these, three monomeric IAP antagonists (**1**–**3**) and one homodimeric antagonist (**4**) are currently under evaluation in clinical trials (Figure 1).[16]

Previously, we reported heterodimeric IAP antagonist **5** (Figure 2) was efficacious in human tumor xenograft models in athymic mice.[17] Here, we describe additional exploratory efforts which have led to the discovery of a series of highly potent truncated linker analogues with improved in vitro antiproliferative activity in a range of human cancer cell lines. Select truncated heterodimers have further shown robust antitumor efficacy in human melanoma and lung cancer xenograft models and represent promising candidates for the treatment of cancer.

CHEMISTRY

The synthesis of novel heterodimeric compounds **6**–**10** is summarized in Scheme 1 and is analogous to that previously reported for **5**.[17] Preparation of **11** resulted from reductive amination of glyoxylic acid with amino-tetrahydroisoquinoline (THIQ) intermediate **19**, followed by amide coupling with aminopyrrolidine **18** and global Boc-deprotection.[18] Urea analogue **12** was prepared in one pot by treatment of **19** with triphosgene, subsequent quenching of the resulting

Received: September 25, 2014

DOI: 10.1021/jm501482t
J. Med. Chem. XXXX, XXX, XXX−XXX

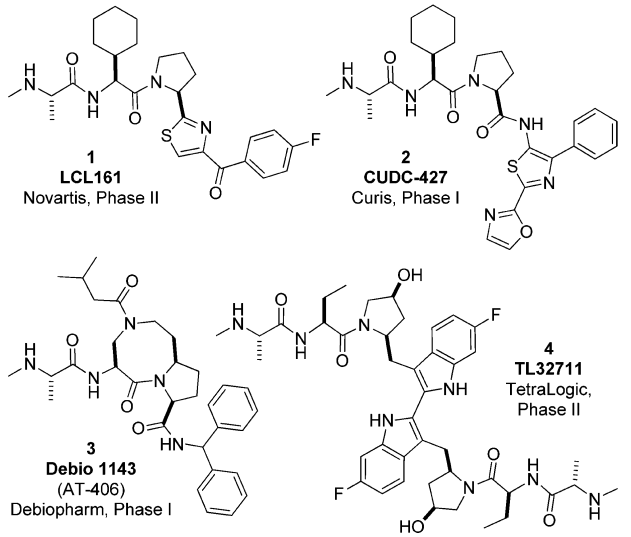

Figure 1. Structures of monomeric and dimeric IAP antagonists in clinical development.

isocyanate intermediate with **18**, and addition of TFA to remove the Boc protecting groups.

Regioisomeric amide derivatives **13** and **14** were accessed as depicted in Scheme 2. Commercially available ketoproline **20** was converted in two steps to enol triflate **21**. Palladium-catalyzed carbonylation was followed by stereoselective reduction of the olefin and concomitant removal of the Cbz group to give **23**. Sequential amino acid couplings with Boc-protected *t*-leucine and then Boc-*N*-Me-L-alanine provided **24**, which was coupled with **19** to give final compound **13** after Boc-deprotection. Starting from hydroxy-THIQ **25**,[19] conversion to the aryl triflate followed by carbonylation and acid-mediated removal of the Boc group gave **26**.[20] As described for **13**, sequential amino acid couplings and Boc-deprotections gave **27** and **28** after hydrolysis of the methyl ester. Final amide coupling with **18** provided **14** after cleavage of the Boc groups.

For the synthesis of truncated linker analogue **15**, reductive amination of keto-proline **29** with amino-THIQ **30** provided stereoselective access to **31** (Scheme 3).[19] Sequential Boc-deprotections and amino acid couplings allowed for elaboration to final compound **15**. Related analogue **16** arose from Mitsunobu coupling of commercially available Boc-L-4-hydroxy-proline methyl ester with hydroxy-THIQ intermediate **25** (ADDP, PPh_3, CH_2Cl_2) followed by chemistry analogous to that described for **15**.[19] As shown in Scheme 4, Suzuki coupling between enol triflate **32** (prepared from **29** according to Scheme 2) and boronate ester **33** provided **34**. Stereoselective hydrogenation of the olefin with Pd/C enabled access to **35**, which was then elaborated to final compound **17**.

Scheme 1. Synthesis of Amino THIQ-Based Analogues 6–12[a]

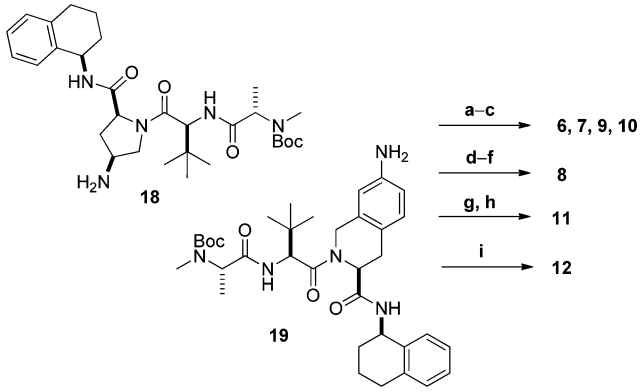

[a]Reagents and conditions: (a) **18**, $MeCO_2$-R-CO_2H, EDC, HOAt, NMM, DMF, rt; (b) NaOH, THF/MeOH, rt; (c) (1) **19**, EDC, HOAt, NMM, DMF, rt, (2) TFA, CH_2Cl_2, rt; (d) **19**, methyl 5-chloro-2,2,3,3,4,4-hexafluoro-5-oxopentanoate, Et_3N, CH_2Cl_2, 0 °C to rt, (e) Ghosez's reagent, **18**, *i*-Pr_2EtN, rt; (f) TFA, CH_2Cl_2, rt; (g) **19**, glyoxylic acid, $Na(OAc)_3BH$, DCE, rt; (h) (1) **18**, EDC, HOAt, NMM, DMF, rt, (2) TFA, CH_2Cl_2, rt; (1) **19**, triphosgene, *i*-Pr_2EtN, CH_2Cl_2, 0 °C, then **18**, *i*-Pr_2EtN, CH_2Cl_2, rt, then TFA.

RESULTS AND DISCUSSION

Compared to monomeric IAP antagonists, dimeric antagonists are reported to more effectively inhibit XIAP due to their ability to simultaneously bind both the BIR2 and BIR3 domains.[21,22] Monomers primarily antagonize the BIR3 domain, as exemplified by GDC-0152,[23] which potenly inhibits XIAP BIR3 (IC_{50} = 18 nM) while lacking affinity for XIAP BIR2–3 (IC_{50} > 800 nM). Although monomeric IAP antagonists induce cell death in a subset of cancer cell lines (e.g., human breast cancer MDA-MB-231; GDC-0152, IC_{50} = 39 nM), the superior affinity of dimeric antagonists for XIAP BIR2–3 results in improved potency and a broader spectrum of antiproliferative activity in some cancer cells that are resistant to monomers (e.g., human melanoma A875; GDC-0152, IC_{50} > 2500 nM vs **4**, IC_{50} = 40 nM).[22,24] Considering the potential of dimeric

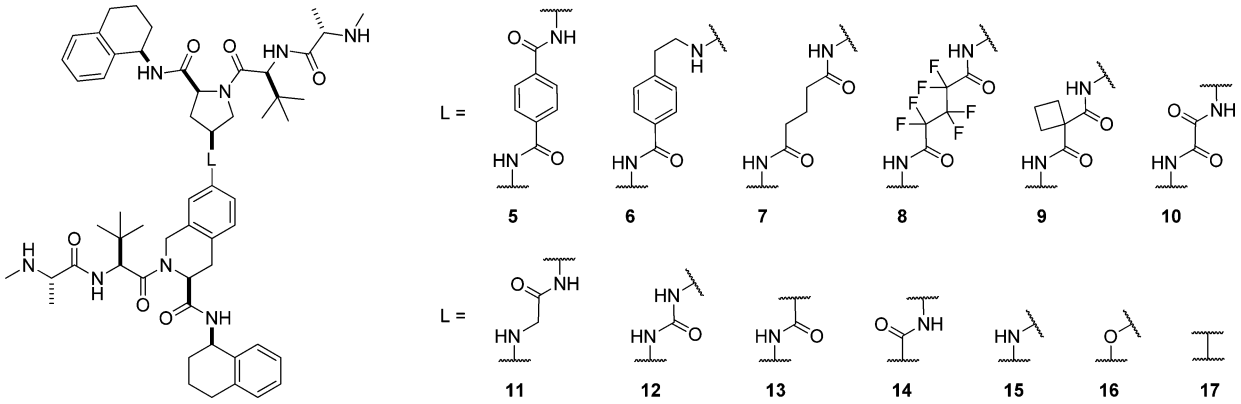

Figure 2. Previously reported IAP antagonist **5** and new heterodimeric compounds **6–17**.

DOI: 10.1021/jm501482t
J. Med. Chem. XXXX, XXX, XXX–XXX

Scheme 2. Synthesis of Regioisomeric Amide Linker Analogues 13 and 14[a]

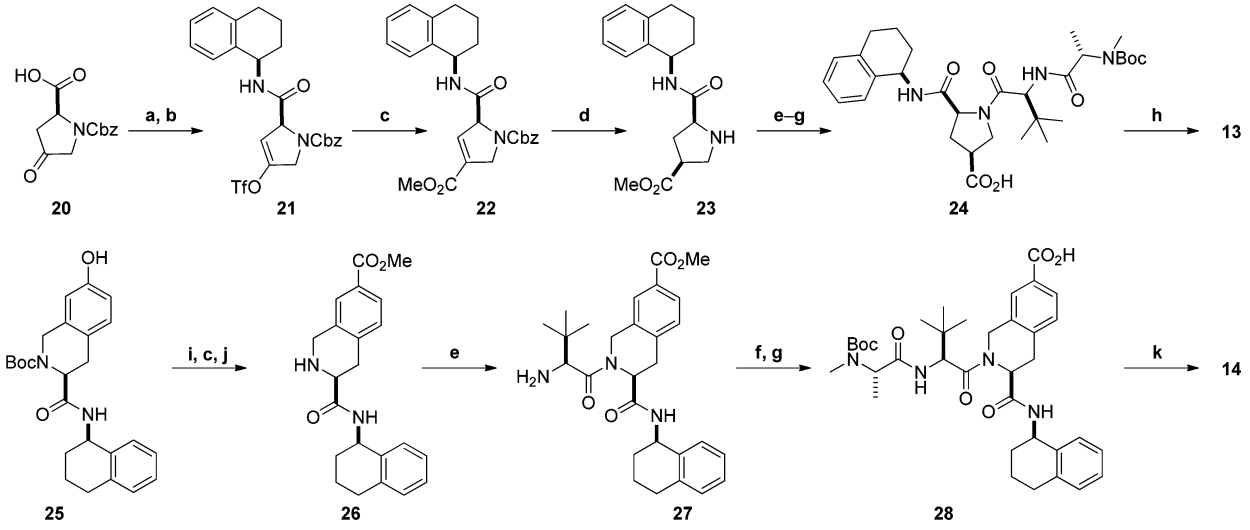

[a]Reagents and conditions: (a) EDC, HOAt, (*R*)-1,2,3,4-tetrahydronaphthalen-1-amine, NMM, DMF, rt; (b) NaHMDS, $PhNTf_2$, THF, −78 °C to −10 °C; (c) $Pd(OAc)_2$, CO, Et_3N, MeOH/DMSO, 70 °C; (d) $Pd(OH)_2$, H_2, MeOH, rt; (e) (1) *N*-Boc-L-*tert*-leucine, EDC, HOAt, NMM, DMF, rt, (2) TFA, CH_2Cl_2, rt; (f) Boc-*N*-methyl-L-alanine, EDC, HOAt, NMM, DMF, rt; (g) NaOH, THF/MeOH, rt; (h) (1) **19**, EDC, HOAt, NMM, DMF, rt, (2) TFA, CH_2Cl_2, rt; (1) $PhNTf_2$, Et_3N, DMAP, CH_2Cl_2, 0 °C to rt; (j) TFA, CH_2Cl_2, rt; (k) (1) **18**, EDC, HOAt, NMM, DMF, rt, (2) TFA, CH_2Cl_2, rt.

Scheme 3. Synthesis of Truncated Linker Analogue 15[a]

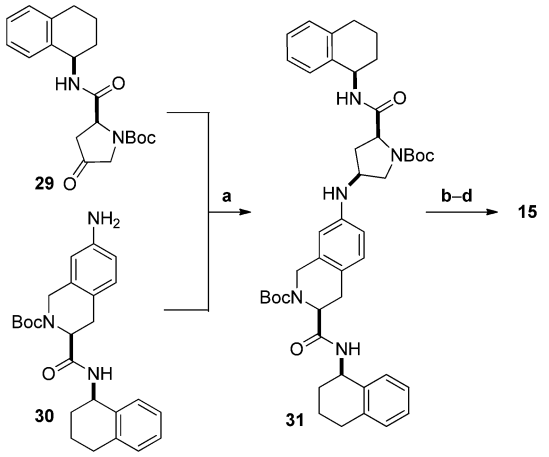

[a]Reagents and conditions: (a) $Na(OAc)_3BH$, AcOH, DCE, rt; (b) TFA, CH_2Cl_2, rt; (c) (1) *N*-Boc-L-*tert*-leucine, EDC, HOAt, NMM, DMF, rt, (2) TFA, CH_2Cl_2, rt; (d) (1) Boc-*N*-methyl-L-alanine, EDC, HOAt, NMM, DMF, rt, (2) TFA, CH_2Cl_2, rt.

Scheme 4. Synthesis of Analogue 17[a]

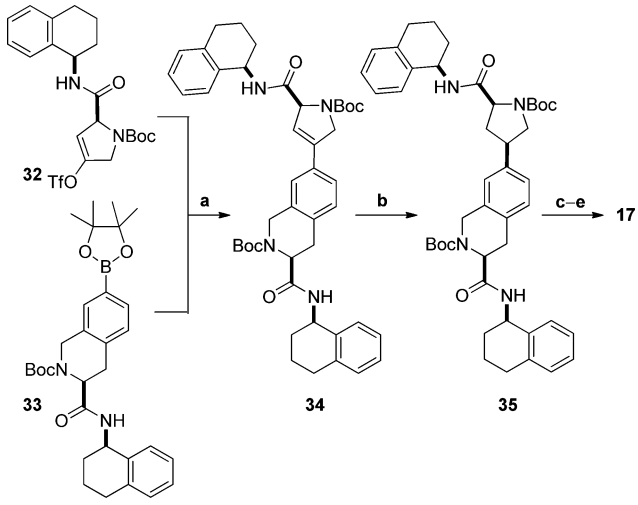

[a]Reagents and conditions: (a) $Pd(PPh_3)_4$, aq Na_2CO_3, dioxane, 100 °C; (b) Pd/C, H_2, MeOH, rt; (c) TFA, CH_2Cl_2, rt; (d) (1) *N*-Boc-L-*tert*-leucine, EDC, HOAt, NMM, DMF, rt, (2) TFA, CH_2Cl_2, rt; (e) (1) Boc-*N*-methyl-L-alanine, EDC, HOAt, NMM, DMF, rt, (2) TFA, CH_2Cl_2, rt.

inhibitors to exhibit improved XIAP activity and impact a wider range of cancer cell types, we sought to identify a potent dimeric antagonist of IAPs for preclinical evaluation.[25]

In general, the linker tethering two monomeric IAP antagonist subunits has been shown to have a minimal effect on cIAP and XIAP binding affinities due to the flexible nature of the peptide between the BIR2 and BIR3 binding domains.[26] However, the linker can profoundly impact the cellular permeability of dimeric compounds and therefore their activity in cell-based assays.[26,27] Tethers of various lengths and polarity were explored to assess the influence of the linker region in the context of the THIQ-based heterodimeric scaffold shown in Figure 2. As expected, little variation was observed in the ability of the compounds to bind human cIAP1- or XIAP BIR2−3 or to restore the activity of caspase-3 in a cell-free functional assay (maximum 6-fold difference, Table 1). Following previous examples that longer, more lipophilic linkers improve cellular potency, we first extended the linker of **5** with an ethyl spacer to give analogue **6**. Unexpectedly, **6** (cLogP = 6.1) showed inferior antiproliferative activity in both MDA-MB-231 and A875 cells, on par with the less lipophilic linker of **7** (cLogP = 4.4).[28] Oxamide **10**, on the other hand, demonstrated significantly improved cellular potency compared to **7** despite its similar cLogP and polar surface area (4.2 and 239, respectively). Attempts to improve cellular permeability by reducing PSA led to urea **12** (PSA = 222) and amide **13** (PSA = 210); both compounds lost potency relative to **10**. Regioisomeric amide **14**, however, was 5-fold more active

DOI: 10.1021/jm501482t
J. Med. Chem. XXXX, XXX, XXX−XXX

Table 1. In Vitro Assessment of IAP Antagonists: Binding Affinities to cIAP1 BIR2−3 and XIAP BIR2−3, Rescue of Caspase-3 Activity, and Cytotoxicity in MDA-MB-231 and A875 Cancer Cell Lines[a]

compd	cIAP1 BIR2−3 IC_{50} (nM)	XIAP BIR2−3 IC_{50} (nM)	caspase-3 activ EC_{50} (nM)	MDA-MB-231 cytotox IC_{50} (nM)	A875 cytotox IC_{50} (nM)
4	50 ± 8.0	126 ± 31	168 (n = 2)	10 (n = 2)	40 (n = 2)
5	10 ± 0.2	4.0 ± 0.0	28 ± 5.7	1.5 ± 0.5	6.8 ± 1.9
6	4.2 ± 1.7	4.7 ± 1.0	10 ± 2.9	4.6 ± 0.5	24 ± 1.2
7	3.4 ± 0.9	3.5 ± 0.7	32 ± 6.1	6.1 ± 1.4	36 ± 6.4
8	17 ± 1.7	6.9 ± 1.3	50 ± 9.3	1.9 ± 0.5	9.7 ± 2.0
9	4.0 ± 0.8	4.0 ± 0.7	17 ± 8.8	2.7 ± 0.4	9.0 ± 0.9
10	4.8 (n = 1)	2.7 ± 0.5	10 ± 2.9	1.3 ± 0.2	6.2 ± 2.0
11	4.7 ± 0.9	7.8 ± 1.0	58 ± 26	8.0 ± 1.4	35 ± 4.2
12	5.6 ± 1.0	3.2 ± 1.1	16 ± 4.5	2.8 ± 0.8	11 ± 1.4
13	2.9 ± 0.8	1.3 ± 0.5	55 ± 24	2.0 ± 0.3	26 ± 2.7
14	4.5 ± 1.7	5.5 ± 0.5	20 ± 6.4	1.2 ± 0.2	4.8 ± 1.7
15	3.4 ± 1.3	2.5 ± 0.2	12 ± 3.7	0.8 ± 0.1	3.0 ± 1.1
16	3.6 ± 0.3	2.3 ± 0.4	31 ± 12	0.9 ± 0.1	8.1 ± 3.5
17	4.9 ± 1.2	1.5 ± 0.4	10 ± 1.6	0.3 ± 0.1	0.8 ± 0.2

[a]Values are reported as mean ± standard deviation calculated from three independent experiments unless otherwise indicated.

than **13** in the A875 cell line. Further shortening the linker gave similarly potent analogues **15** and **16**. Encouraged by the antiproliferative activity of these truncated linker analogues, we removed the linker entirely to give **17**, which gratifyingly displayed subnanomolar activity in both cancer cell lines.

Despite similar binding affinities for cIAP1 BIR2−3 and XIAP BIR2−3, the antagonists exhibited considerable differences in their kinetics of binding. For example, the rate of dissociation (k_{off}) from XIAP BIR2−3 for **15** ($t_{1/2}$ = 58 min) was slower than **5** ($t_{1/2}$ = 19 min), while no detectable off-rate was observed for **17** ($t_{1/2}$ > 3 h).[29] Similar off-rates were observed for these compounds from cIAP1 BIR2−3.

With the goal of identifying a broad spectrum IAP antagonist, we were particularly encouraged by the potent antiproliferative activity of the truncated heterodimers in the XIAP-dependent A875 melanoma cell line. To evaluate whether this potency would translate in vivo, pharmacokinetic (PK) screening of analogues **14**−**17** in mice (1 mg/kg dose) was used to guide selection of appropriate compounds for efficacy studies. While low serum exposure of **16** (AUC = 29 nM·h) precluded its advancement, **14**, **15**, and **17** demonstrated acceptable PK profiles (AUCs ∼1 μM·h) and were selected for testing in the A875 human tumor xenograft model. As shown in Table 2, intravenous treatment with **14**, **15**, or **17** resulted in complete tumor regressions at a 1 mg/kg dose, with no detectable tumor regrowth even after dosing ceased in at least 4 out of 8 mice. All compounds were well-tolerated, with no overt signs of toxicity or weight loss. At the same dose, homodimeric clinical candidate **4** was inactive in this model, presumably due to its decreased ability to inhibit XIAP.[30]

Table 2. Antitumor Activity of IAP Antagonists in the A875 Xenograft Model in Implanted Mice[a]

compd	mean TGI (%)	cures	average weight change (%)
4	15	0 of 8	−1.8
5	100	2 of 8	−3.0
14	103	4 of 8	−0.2
15	100	4 of 8	2.1
17	112	7 of 8	4.5

[a]Compounds were administered intravenously (iv) at 1 mg/kg every 3 days for 6 doses, 8 animals per group. See Supporting Information for calculation of TGI. Cures are defined as no measurable tumor for 10 tumor volume doubling times after dosing has ceased. Weight change is maximum recorded weight gain or loss.

Several truncated heterodimers were further profiled in a small panel of human lung cancer cell lines. Among these, **15** and **17** demonstrated highly potent antiproliferative activity in H1703 cells (IC_{50}s < 1 nM). In an H1703 xenograft model, **15** and **17** exhibited dose-dependent inhibition of tumor growth (Figure 3). Although both compounds were inactive at the lowest dose, tumor regressions were observed at the maximum tolerated dose (MTD) of **15** (15 mg/kg, 108% TGI) and at the 5 and 7.5 mg/kg doses of **17** (113 and 124% TGI, respectively). Notably, tumors were undetectable in 3 of the 8 mice in the 7.5 mg/kg (MTD) group following treatment with **17**. The exceptionally slow k_{off} previously observed for **17** may contribute to its superior in vivo efficacy.

CONCLUSIONS

Prompted by the potential of targeting IAPs for the treatment of various malignancies, we pursued a dimeric antagonist of IAPs for application to a range of human cancers. Exploring modifications to the linker region of **5** revealed that shortening the linker improved antiproliferative activity in cIAP- and XIAP-dependent cell lines. Several truncated heterodimers further demonstrated curative efficacy without weight loss in the A875 xenograft model. At higher doses, **15** and **17** induced complete tumor regressions in a lung cancer xenograft model. Combined, these results support the advancement of **15** and **17** to exploratory toxicology studies to determine the optimal candidate for advanced preclinical development.

EXPERIMENTAL SECTION

General. All final compounds were isolated in ≥95% purity as assessed by analytical reverse phase HPLC (see Supporting Information for details).

General Procedure for Amide Coupling. To a 0 °C solution of carboxylic acid (2.0 equiv) in DMF (0.15 M) was added EDC (2.4 equiv) followed by HOAt (2.4 equiv). After 10 min, amine (1.0 equiv) and NMM (6.0 equiv) were added. The resulting reaction mixture was allowed to warm to rt overnight and then poured into a separatory funnel containing EtOAc and satd aq $NaHCO_3$. The aqueous layer was extracted with EtOAc (3×). The combined organic extracts were washed with 1 N HCl, 10% LiCl, and satd NaCl and then dried over Na_2SO_4, filtered, and concentrated in vacuo.

DOI: 10.1021/jm501482t
J. Med. Chem. XXXX, XXX, XXX−XXX

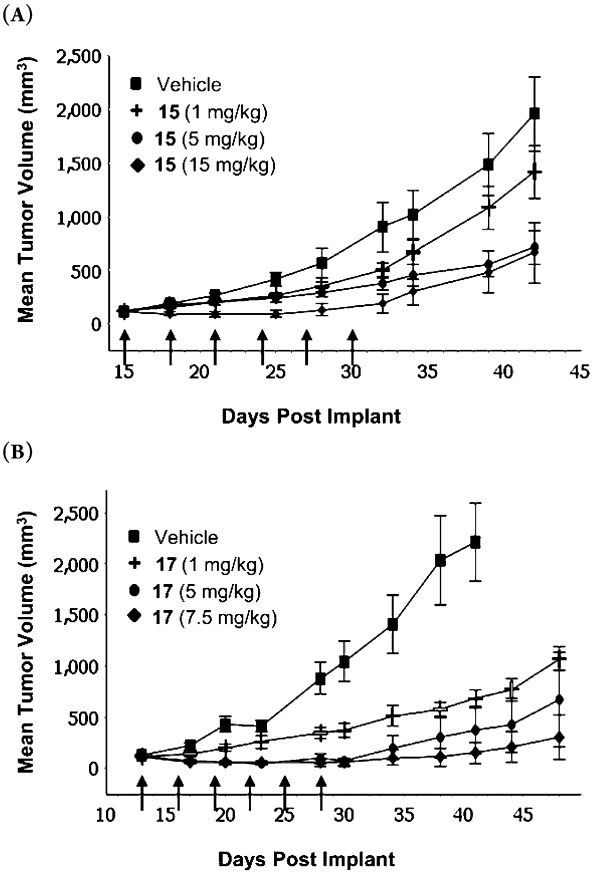

Figure 3. Antitumor activity of **15** (A) and **17** (B) in the H1703 xenograft model in mice. Compounds were administered intravenously (iv) every 3 days for 6 doses (on days indicated by arrows) with 8 animals per group.

General Procedure for *N*-Boc Deprotection. To a solution of Boc-protected amine (1.0 equiv) in CH_2Cl_2 (0.2 M) was added TFA (20 equiv). The resulting reaction mixture was stirred at rt for 1 h and then quenched with satd aq $NaHCO_3$. The aqueous layer was extracted with EtOAc (3×), and the combined organic extracts were washed with satd NaCl, dried over Na_2SO_4, filtered, and concentrated in vacuo.

(*S*)-*tert*-Butyl 7-(((3*S*,5*S*)-1-(*tert*-Butoxycarbonyl)-5-(((*R*)-1,2,3,4-tetrahydronaphthalen-1-yl)carbamoyl)pyrrolidin-3-yl)-amino)-3-(((*R*)-1,2,3,4-tetrahydronaphthalen-1-yl)carbamoyl)-3,4-dihydroisoquinoline-2(1*H*)-carboxylate (31). To a solution of ketone **29** (9.35 g, 26.1 mmol) and aniline **30** (10.0 g, 23.7 mmol) in DCE (100 mL) were added AcOH (2.0 mL, 35.6 mmol) and dried 4 Å molecular sieves (~3 g). The reaction mixture was stirred at rt for 2 h and then $Na(OAc)_3BH$ (10.0 g, 47.4 mmol) was added in three portions, 30 min apart. The resulting reaction mixture was stirred at rt overnight and then quenched by adding satd aq $NaHCO_3$ (~60 mL). The mixture was extracted with CH_2Cl_2 (3×). The combined organic extracts were washed with satd NaCl, dried over Na_2SO_4, filtered, and concentrated in vacuo. The crude solid was purified using flash column chromatography (gradient 0−10% acetone/CH_2Cl_2) to give **31** (13.9 g, 72%) as a pale-orange solid. ^{1}H NMR (400 MHz, CD_3OD, mixture of amide rotamers) δ 7.42−7.20 (m, 1H), 7.17−6.91 (m, 8H), 6.60 (d, J = 7.5 Hz, 1H), 6.46 (br s, 1H), 5.11−5.02 (m, 1H), 4.93 (br s, 1H), 4.75−4.56 (m, 1H), 4.54−4.44 (m, 1H), 4.40−4.23 (m, 2H), 4.07 (br s, 1H), 3.84 (br s, 1H), 3.45−3.37 (m, 1H), 3.18−2.98 (m, 2H), 2.89−2.68 (m, 4H), 2.59 (br s, 1H), 2.05−1.63 (m, 9H), 1.55−1.40 (m, 18H). MS (ESI$^+$) m/z 764.6 (M + H)$^+$.

(*S*)-2-((*S*)-3,3-Dimethyl-2-((*S*)-2-(methylamino)-propanamido)butanoyl)-7-(((3*S*,5*S*)-1-((*S*)-3,3-dimethyl-2-((*S*)-2-(methylamino)propanamido)butanoyl)-5-(((*R*)-1,2,3,4-tetrahydronaphthalen-1-yl)carbamoyl)pyrrolidin-3-yl)amino)-*N*-((*R*)-1,2,3,4-tetrahydronaphthalen-1-yl)-1,2,3,4-tetrahydroisoquinoline-3-carboxamide, 2 HCl (15). Following the general procedure for *N*-Boc deprotection, **31** (13.9 g, 18.2 mmol) was converted to a crude oil. Following the general procedure for amide coupling, the crude oil and *N*-Boc-L-*tert*-leucine (8.66 g, 37.4 mmol) were converted to Boc-precursor I (14.8 g, 82%) after purification using flash column chromatography (gradient 0−40% EtOAc/CH_2Cl_2). MS(ESI$^+$) m/z 990.8 (M + H)$^+$.

Following the general procedure for *N*-Boc deprotection, Boc-precursor I (14.8 g, 15.0 mmol) was converted to a crude bis-amine. Following the general procedure for amide coupling, the crude bis-amine and Boc-*N*-methyl-L-alanine (6.34 g, 31.2 mmol) were converted to Boc-precursor II (15.1 g, 87%) after purification using flash column chromatography (gradient 0−60% EtOAc/CH_2Cl_2). MS(ESI$^+$) m/z 1161.0 (M + H)$^+$.

A solution of TFA (5.0 mL) in CH_2Cl_2 (15.0 mL) was added to Boc-precursor II (4.30 g, 3.73 mmol) at 0 °C. The resulting reaction mixture was warmed to rt, stirred for 2.5 h, and then concentrated in vacuo. Et_2O (15 mL) was added to the residue, and the resulting solid was collected by filtration. The solid was dissolved in EtOAc (80 mL) and washed with 0.5 N NaOH (5 × 20 mL) and then with water (20 mL). The organic layer was dried over $MgSO_4$, filtered, and concentrated in vacuo. To a suspension of the resulting solid in water (12 mL) at 0 °C was added 1 N HCl (16 mL) dropwise over 15 min. The homogeneous solution was stirred at 0 °C for 15 min, then at rt for 15 min, and lyophilized to give **15** (3.3 g, 92%) as a white solid. ^{1}H NMR (500 MHz, DMSO-d_6, mixture of amide rotamers) δ 9.76−9.55 (m, 2H), 8.91 (br s, 2H), 8.77 (d, J = 7.5 Hz, 1H), 8.69 (d, J = 8.1 Hz, 1H), 8.69−8.65 (m, 1H), 8.65 (d, J = 8.5 Hz, 1H), 8.22 (d, J = 8.8 Hz, 1H), 7.33 (d, J = 7.5 Hz, 1H), 7.08 (dd, J = 2.3, 0.6 Hz, 10H), 5.01 (br s, 1H), 5.00 (br s, 1H), 4.97 (d, J = 8.8 Hz, 1H), 4.88 (d, J = 7.5 Hz, 1H), 4.86 (br s, 1H), 4.70 (t, J = 6.6 Hz, 1H), 4.62 (d, J = 14.9 Hz, 1H), 4.46 (d, J = 7.9 Hz, 1H), 4.17 (d, J = 5.3 Hz, 1H), 4.08 (d, J = 5.8 Hz, 1H), 4.00−3.96 (m, 2H), 3.78 (br s, 1H), 2.99 (br s, 1H), 2.78−2.74 (m, 1H), 2.66 (br s, 4H), 2.50 (br s, 1H), 2.46−2.39 (m, 6H), 1.90 (d, J = 2.8 Hz, 1H), 1.89−1.82 (m, 2H), 1.73 (d, J = 23.1 Hz, 4H), 1.69−1.50 (m, 2H), 1.34 (d, J = 6.8 Hz, 3H), 1.27 (d, J = 6.8 Hz, 3H), 1.08 (s, 9H), 1.03 (s, 9H). HRMS (ESI$^+$) m/z calcd for $C_{55}H_{78}N_9O_6$ (M+H)$^+$: 960.60696, obsd 960.60526.

(*S*)-*tert*-Butyl 7-((*S*)-1-(*tert*-Butoxycarbonyl)-5-(((*R*)-1,2,3,4-tetrahydronaphthalen-1-yl)carbamoyl)-2,5-dihydro-1*H*-pyrrol-3-yl)-3-(((*R*)-1,2,3,4-tetrahydronaphthalen-1-yl)carbamoyl)-3,4-dihydroisoquinoline-2(1*H*)-carboxylate (34). A solution of triflate **32** (2.82 g, 5.75 mmol), boronate ester **33** (3.21 g, 6.04 mmol), and 2 M Na_2CO_3 (7.2 mL, 14.4 mmol) in dioxane (50 mL) was degassed with Ar. $Pd(PPh_3)_4$ (450 mg, 0.39 mmol) was added, and the orange reaction mixture was stirred at 95 °C for 3 h and then poured into a separatory funnel containing satd NH_4Cl. The aqueous layer was extracted with EtOAc (3×). The combined organic extracts were washed with satd NaCl and dried over Na_2SO_4. Filtration and concentration in vacuo gave a crude oil which was purified using flash column chromatography (gradient 0−100% EtOAc/hexanes) and then repurified (gradient 0−60% EtOAc, then isocratic at 60% EtOAc/hexanes) to give **34** (3.84 g, 90%) as an off-white oily solid. ^{1}H NMR (500 MHz, DMSO-d_6, mixture of amide rotamers) δ 8.48−8.32 (m, 1H), 8.04−7.85 (m, 1H), 7.44−7.30 (m, 2H), 7.29−7.18 (m, 2H), 7.18−7.07 (m, 3H), 7.07−6.97 (m, 2H), 6.86 (br s, 1H), 6.43 (br d, J = 6.7 Hz, 1H), 6.29−6.14 (m, 1H), 5.08−4.90 (m, 2H), 4.86−4.67 (m, 1H), 4.53 (br s, 3H), 4.49−4.35 (m, 2H), 3.22−2.98 (m, 2H), 2.83−2.57 (m, 4H), 1.98−1.82 (m, 3H), 1.81−1.59 (m, 5H), 1.52−1.35 (m, 18H). MS(ESI$^+$) m/z 747.5 (M + H)$^+$.

(*S*)-*tert*-Butyl 7-((3*R*,5*S*)-1-(*tert*-Butoxycarbonyl)-5-(((*R*)-1,2,3,4-tetrahydronaphthalen-1-yl)carbamoyl)pyrrolidin-3-yl)-3-(((*R*)-1,2,3,4-tetrahydronaphthalen-1-yl)carbamoyl)-3,4-dihydroisoquinoline-2(1*H*)-carboxylate (35). To a 500 mL pressure flask containing 5% Pd/C (1.09 g, 0.51 mmol) was added a solution of **34** (3.84 g, 5.14 mmol) in MeOH (20 mL). The resulting reaction mixture was stirred under 25 psi H_2 overnight and then filtered through a pad of Celite washing with EtOAc. The filtrate was concentrated in vacuo and purified using flash column chromatog-

DOI: 10.1021/jm501482t
J. Med. Chem. XXXX, XXX, XXX−XXX

raphy (gradient 0−90% EtOAc/hexanes) to give **35** (2.41 g, 63%). ^{1}H NMR (500 MHz, DMSO-d_6) δ 8.34−8.21 (m, 1H), 8.10−7.79 (m, 1H), 7.38−7.28 (m, 1H), 7.22 (br d, J = 7.3 Hz, 1H), 7.17−7.01 (m, 7H), 6.96−6.83 (m, 1H), 6.62−6.38 (m, 1H), 4.97 (br s, 1H), 4.81 (br s, 1H), 4.59−4.38 (m, 2H), 4.32−4.15 (m, 1H), 3.97−3.76 (m, 1H), 3.30−3.22 (m, 4H), 3.19−2.95 (m, 2H), 2.81−2.57 (m, 5H), 1.86 (br s, 4H), 1.75−1.55 (m, 4H), 1.52−1.32 (m, 18H). MS(ESI$^+$) m/z 749.5 $(M + H)^+$.

(*S*)-2-((*S*)-3,3-Dimethyl-2-((*S*)-2-(methylamino)-propanamido)butanoyl)-7-((3*R*,5*S*)-1-((*S*)-3,3-dimethyl-2-((*S*)-2-(methylamino)propanamido)butanoyl)-5-(((*R*)-1,2,3,4-tetrahydronaphthalen-1-yl)carbamoyl)pyrrolidin-3-yl)-*N*-((*R*)-1,2,3,4-tetrahydronaphthalen-1-yl)-1,2,3,4-tetrahydroisoquinoline-3-carboxamide, 2 HCl (17). Following the general procedure for *N*-Boc deprotection, **35** (1.10 g, 1.47 mmol) was converted to a crude oil. Following the general procedure for amide coupling, the crude oil and *N*-Boc-L-*tert*-leucine (644 mg, 2.78 mmol) were converted to Boc-precursor I (945 mg, 66%) after purification using flash column chromatography (gradient 0−100% EtOAc/hexanes). MS(ESI$^+$) m/z 975.6 $(M + H)^+$.

Following the general procedure for *N*-Boc deprotection, Boc-precursor I (1.05 g, 1.08 mmol) was converted to a crude bis-amine. Following the general procedure for amide coupling, the crude bis-amine and Boc-*N*-methyl-L-alanine (450 mg, 2.22 mmol) were converted to Boc-precursor II (0.99 g, 82%) after purification using flash column chromatography (gradient 0−80% EtOAc/CH_2Cl_2). MS(ESI$^+$) m/z 1146.2 $(M + H)^+$.

To a solution of Boc-precursor II (447 mg, 0.39 mmol) in CH_2Cl_2 (5.0 mL) was added TFA (1.5 mL). The reaction mixture was stirred at rt for 1 h, then concentrated in vacuo, purified by preparative HPLC, and lyophilized. The resulting white solid was dissolved in EtOAc (50 mL), washed with 1N NaOH (3 × 10 mL) and water (5 mL) and then dried over $MgSO_4$. Filtration and concentration in vacuo gave **17** (free base, 265 mg, 72%) as a white solid. To a suspension of **17** (free base, 120 mg, 0.13 mmol) in water (5.0 mL) at 0 °C was added 1 N HCl (0.64 mL, 0.64 mmol) dropwise. The resulting clear solution was stirred at rt for 20 min and then lyophilized give **17** (2 HCl, 115 mg, 88%) as a white solid. ^{1}H NMR (500 MHz, DMSO-d_6, mixture of amide rotamers) δ 9.33 (br s, 2H), 8.86 (br s, 2H), 8.72−8.62 (m, 2H), 8.50 (d, J = 8.8 Hz, 1H), 8.13 (d, J = 8.8 Hz, 1H), 7.39 (d, J = 7.9 Hz, 1H), 7.26 (s, 1H), 7.22 (s, 1H), 7.19 (s, 1H), 7.16−7.10 (m, 2H), 7.11−7.02 (m, 3H), 6.99 (t, J = 7.6 Hz, 1H), 6.92 (d, J = 7.7 Hz, 1H), 5.01 (d, J = 9.0 Hz, 1H), 5.00−4.93 (m, 1H), 4.90−4.82 (m, 2H), 4.78 (t, J = 6.2 Hz, 1H), 4.75−4.69 (m, 1H), 4.57 (d, J = 8.3 Hz, 1H), 4.47−4.40 (m, 1H), 4.28 (t, J = 8.5 Hz, 1H), 3.97 (d, J = 5.1 Hz, 2H), 3.52−3.43 (m, 1H), 3.42−3.36 (m, 1H), 3.06 (d, J = 6.2 Hz, 2H), 2.78−2.67 (m, 4H), 2.56−2.50 (m, 1H), 2.50−2.44 (m, 6H), 2.01−1.91 (m, 1H), 1.90−1.83 (m, 1H), 1.80−1.73 (m, 1H), 1.72−1.65 (m, 2H), 1.65−1.59 (m, 1H), 1.63−1.56 (m, 2H), 1.58−1.52 (m, 1H), 1.35 (d, J = 6.8 Hz, 3H), 1.29 (d, J = 7.0 Hz, 3H), 1.09 (s, 9H), 1.05 (s, 9H); HRMS (ESI$^+$) m/z calcd for $C_{55}H_{77}N_8O_6$ $(M + H)^+$: 945.59668, obsd 945.59463.

■ ASSOCIATED CONTENT

Ⓢ Supporting Information

General methods, full experimental procedures for **15** and **17**, and characterization data for all new compounds; procedures for binding assays, caspase-3 rescue assay, MDA-MB-231 and A875 cell proliferation assays; pharmacokinetic experiments; tumor growth inhibition and body weight change graphs for in vivo efficacy studies and charaterization of **17** by Western blot. This material is available free of charge via the Internet at http://pubs.acs.org.

■ AUTHOR INFORMATION

Corresponding Author

*Phone: (609) 252-4850. E-mail: heidi.perez@bms.com.

Author Contributions

All authors have given approval to the final version of the manuscript.

Notes

The authors declare no competing financial interest.

■ ACKNOWLEDGMENTS

We thank Robert Schmidt, Chunlei Wang, and Yingru Zhang for purification and analytical support; Gregory Locke for completion of cIAP1 assays, and Henry Shen for caspase-3 rescue assays; Robin Moore, Georgia Cornelius, and Celia D'Arienzo for bioanalytical support; and Anuradha Gupta, Thirupala Reddy, Arun Akunuri, Manivel Pitchai, Rick Rampulla, and Arvind Mathur for contributions to the synthesis of **17**.

■ ABBREVIATIONS USED

IAP, inhibitor of apoptosis protein; BIR, baculovirus inhibitor of apoptosis repeat; XIAP, X-linked inhibitor of apoptosis protein; cIAP, cellular inhibitor of apoptosis; TNF, tumor necrosis factor; RIP, receptor-interacting protein; NIK, NF-κB-inducing kinase; Smac, second mitochondria-derived activator of caspases; DIABLO, direct IAP-binding protein with low p*I*; THIQ, tetrahydroisoquinoline; EDC, *N*-(3-(dimethylamino)-propyl)-*N*′-ethylcarbodiimide hydrochloride; HOAt, 1-hydroxy-7-azabenzotriazole; NMM, *N*-methylmorpholine; DMF, dimethyl formamide; rt, room temperature; THF, tetrahydrofuran; TFA, trifluoroacetic acid; DCE, dichloroethane; Boc, *tert*-butyloxycarbonyl; NaHMDS, sodium bis(trimethylsilyl)-amide; $PhNTf_2$, *N*-phenyl-bis(trifluoromethanesulfonimide); DMSO, dimethyl sulfoxide; *N*-Boc-L-*tert*-leucine, (*S*)-2-((*tert*-butoxycarbonyl)amino)-3,3-dimethylbutanoic acid; Boc-*N*-methyl-L-alanine, (*S*)-2-((*tert*-butoxycarbonyl)(methyl)amino)-propanoic acid; DMAP, 4-(dimethylamino)pyridine; ADDP, 1,1′-(azodicarbonyl)-dipiperidine; PSA, polar surface area; PK, pharmacokinetic; TGI, tumor growth inhibition

■ REFERENCES

(1) Elmore, S. Apoptosis: a review of programmed cell death. *Toxicol. Pathol.* **2007**, *35*, 495−516.

(2) Igney, F. H.; Krammer, P. H. Death and anti-death: tumor resistance to apoptosis. *Nature Rev. Cancer* **2002**, *2*, 277−288.

(3) Fesik, S. W. Promoting apoptosis as a strategy for cancer drug discovery. *Nature Rev. Cancer* **2005**, *5*, 876−885.

(4) Salvensen, G. S.; Duckett, C. S. IAP proteins: blocking the road to death's door. *Nature Rev. Mol. Cell Biol.* **2002**, *3*, 401−410.

(5) Shiozaki, E. N.; Chai, J.; Rigotti, D. J.; Riedl, S. J.; Li, P.; Srinivasula, S. M.; Alnemri, E. S.; Fairman, R.; Shi, Y. Mechanism of XIAP-mediated inhibition of caspase-9. *Mol. Cell* **2003**, *11*, 519−527.

(6) Scott, F. L.; Denault, J.-B.; Riedl, S. J.; Shin, H.; Renatus, M.; Salvesen, G. S. XIAP inhibits caspase-3 and -7 using two bindingsites: evolutionarily conserved mechanism of IAPs. *EMBO J.* **2005**, *24*, 645−655.

(7) Wang, C. Y.; Mayo, M. W.; Korneluk, R. G.; Goeddel, D. V.; Baldwin, A. S. NFκB antiapoptosis: induction of TRAF1 and TRAF2 and c-IAP1 and c-IAP2 to suppress caspase-8 activation. *Science* **1998**, *281*, 1680−1683.

(8) Gyrd-Hansen, M.; Meier, P. IAPs: from caspase inhibitors to modulators of NF-kappaB, inflammation and cancer. *Nature Rev. Cancer* **2010**, *10*, 561−574.

(9) Du, C.; Fang, M.; Li, Y.; Li, L.; Wang, X. Smac, a mitochondrial protein that promotes cytochrome c-dependent caspase activation by eliminating IAP inhibition. *Cell* **2000**, *102*, 33−42.

(10) Verhagen, A. M.; Ekert, P. G.; Pakusch, M.; Silke, J.; Connolly, L. M.; Reid, G. E.; Moritz, R. L.; Simpson, R. J.; Vaux, D. L.

DOI: 10.1021/jm501482t
J. Med. Chem. XXXX, XXX, XXX−XXX

Identification of DIABLO, a mammalian protein that promotes apoptosis by binding to and antagonizing IAP proteins. *Cell* **2000**, *102*, 43−53.
(11) Wu, G.; Chai, J.; Suber, T. L.; Wu, J.-W.; Du, C.; Wang, X.; Shi, Y. Structural basis of IAP recognition by Smac/DIABLO. *Nature* **2000**, *408*, 1008−1012.
(12) Gao, Z.; Tian, Y.; Wang, J.; Yin, Q.; Wu, H.; Li, Y. M.; Jiang, X. A dimeric Smac/Diablo peptide directly relieves caspase-3 inhibition by XIAP. Dynamic and cooperative regulation of XIAP by Smac/Diablo. *J. Biol. Chem.* **2007**, *282*, 30718−30727.
(13) Temesgen, S.; Welsh, K.; Lober, T.; Togo, S. H.; Zapata, J. M.; Reed, J. C. Distinct BIR domains of cIAP1 mediate binding to and ubiquitination of tumor necrosis factor receptor-associated factor 2 and second mitochondrial activator of caspases. *J. Biol. Chem.* **2006**, *281*, 1080−1090.
(14) Tamm, I.; Kornblau, S. M.; Segall, H.; Krajewski, S.; Welsh, K.; Kitada, S.; Scudiero, D. A.; Tudor, G.; Qui, Y. H.; Monks, A.; Andreeff, M.; Reed, J. C. Expression and prognostic significance of IAP-family genes in human cancers and myeloid leukemias. *Clin. Cancer Res.* **2000**, *6*, 1796−1803.
(15) Dubrez, L.; Berthelet, J.; Glorian, V. IAP proteins as targets for drug development in oncology. *OncoTargets Ther.* **2013**, *6*, 1285−1304.
(16) Bai, L.; Smith, D. C.; Wang, S. Small-molecule SMAC mimetics as new cancer therapeutics. *Pharmacol. Ther.* **2014**, *144*, 82−95.
(17) Kim, K. S.; Zhang, L.; Williams, D.; Perez, H. L.; Stang, E.; Borzilleri, R. M.; Posy, S.; Lei, M.; Chaudhry, C.; Emanuel, S.; Talbott, R. Discovery of tetrahydroisoquinoline-based bivalent heterodimeric IAP antagonists. *Bioorg. Med. Chem. Lett.* **2014**, *24*, 5022−5029.
(18) Borzilleri, R. M.; Kim, K. S.; Perez, H. L.; Stang, E. M.; Williams, D. K.; Zhang, L. Preparation of peptide IAP antagonists for cancer treatment. PCT Int. Appl. 047024, 2014.
(19) Borzilleri, R. M.; Perez, H. L.; Stang, E. M.; Kim, K. S. Preparation of peptide IAP antagonists for cancer treatment. U.S. Patent Appl. 0338081, 2013.
(20) Grimm, J. B.; Wilson, K. J.; Witter, D. J. Suppression of racemization in the carbonylation of amino acid derived aryl triflates. *Tetrahedron Lett.* **2007**, *48*, 4509−4513.
(21) Li, L.; Thomas, R. M.; Suzuki, H.; De Brabander, J. K.; Wang, X.; Harran, P. G. A small molecule Smac mimic potentiates TRAIL- and TNFalpha-mediated cell death. *Science* **2004**, *305*, 1471−1474.
(22) Lu, J.; Bai, L.; Sun, H.; Nikolovska-Coleska, Z.; McEachern, D.; Qiu, S.; Miller, R. S.; Yi, H.; Shangary, S.; Sun, Y.; Meagher, J. L.; Stuckey, J. A.; Wang, S. SM-164: a novel, bivalent Smac mimetic that induces apoptosis and tumor regression by concurrent removal of the blockade of cIAP-1/2 and XIAP. *Cancer Res.* **2008**, *68*, 9384−9393.
(23) Flygare, J. A.; Beresini, M.; Budha, N.; Chan, H.; Chan, I. T.; Cheeti, S.; Cohen, F.; Deshayes, K.; Doerner, K.; Eckhardt, S. G.; Elliott, L. O.; Feng, B.; Franklin, M. C.; Reisner, S. F.; Gazzard, L.; Halladay, J.; Hymowitz, S. G.; La, H.; LoRusso, P.; Maurer, B.; Murray, L.; Plise, E.; Quan, C.; Stephan, J. P.; Young, S. G.; Tom, J.; Tsui, V.; Um, J.; Varfolomeev, E.; Vucic, D.; Wagner, A. J.; Wallweber, H. J.; Wang, L.; Ware, J.; Wen, Z.; Wong, H.; Wong, J. M.; Wong, M.; Wong, S.; Yu, R.; Zobel, K.; Fairbrother, W. J. Discovery of a potent small-molecule antagonist of inhibitor of apoptosis (IAP) proteins and clinical candidate for the treatment of cancer (GDC-0152). *J. Med. Chem.* **2012**, *55*, 4101−4113.
(24) Jost, P. J.; Grabow, S.; Gray, D.; McKenzie, M. D.; Nachbur, U.; Huang, D. C. S.; Bouillet, P.; Thomas, H. E.; Borner, C.; Silke, J.; Strasser, A.; Kaufmann, T. XIAP discriminates between type I and type II FAS-induced apoptosis. *Nature* **2009**, *460*, 1035−1039.
(25) Ndubaku, C.; Varfolomeev, E.; Wang, L.; Zobel, K.; Lau, K.; Elliott, L. O.; Maurer, B.; Fedorova, A. V.; Dynek, J. N.; Koehler, M.; Hymowitz, S. G.; Tsui, V.; Deshayes, K.; Fairbrother, W. J.; Flygare, J. A.; Vucic, D. Antagonism of c-IAP and XIAP proteins is required for efficient induction of cell death by small-molecule IAP antagonists. *ACS Chem. Biol.* **2009**, *4*, 557−566.
(26) Sun, H.; Liu, L.; Lu, J.; Bai, L.; Li, X.; Nikolovska-Coleska, Z.; McEachern, D.; Yang, C.-Y.; Qiu, S.; Yi, H.; Sun, D.; Wang, S. Potent bivalent Smac mimetics: effect of the linker on binding to inhibitor of apoptosis proteins (IAPs) and anticancer activity. *J. Med. Chem.* **2011**, *54*, 3306−3318.
(27) Hennessy, E. J.; Adam, A.; Aquila, B. M.; Castriotta, L. M.; Cook, D.; Hattersley, M.; Hird, A. W.; Huntington, C.; Kamhi, V. M.; Laing, N. M.; Li, D.; MacIntyre, T.; Omer, C. A.; Oza, V.; Patterson, T.; Repik, G.; Rooney, M. T.; Saeh, J. C.; Sha, L.; Vasbinder, M. M.; Wang, H.; Whitston, D. Discovery of a novel class of dimeric Smac mimetics as potent IAP antagonists resulting in a clinical candidate for the treatment of cancer (AZD5582). *J. Med. Chem.* **2013**, *56*, 9897−9919.
(28) Experimental difficulties precluded obtaining accurate log *D* measurements; cLogP values were calculated using ACD/Laboratories software (v. 12.01, 1997−2010, Advanced Chemistry Development, Inc.).
(29) Chaudhry, C.; et al. Building TR-FRET assays for thermodynamic and kinetic characterization of potent bivalent inhibitors of an IAP-target. Manuscript in preparation.
(30) Condon, S. M.; Mitsuuchi, Y.; Deng, Y.; LaPorte, M. G.; Rippin, S. R.; Haimowitz, T.; Alexander, M. D.; Kumar, P. T.; Hendi, M. S.; Lee, Y. H.; Benetatos, C. A.; Yu, G.; Kapoor, G. S.; Neiman, E.; Seipel, M. E.; Burns, J. M.; Graham, M. A.; McKinlay, M. A.; Li, X.; Wang, J.; Shi, Y.; Feltham, R.; Bettjeman, B.; Cumming, M. H.; Vince, J. E.; Khan, N.; Silke, J.; Day, C. L.; Chunduru, S. K. Birinapant, a Smac-mimetic with improved tolerability for the treatment of solid tumors and hematological malignancies. *J. Med. Chem.* **2014**, *57*, 3666−3677.

DOI: 10.1021/jm501482t
J. Med. Chem. XXXX, XXX, XXX−XXX